Transactions, SMiRT-22
San Francisco, California, USA - August 18-23, 2013
Division IX (include assigned division number from I to X)

INFLUENCE OF HYDROGEN CONTENT ON FRACTURE TOUGHNESS OF HEAT-TREATED Zr-2.5Nb ALLOY

A. K. Bind, R. N. Singh*, J. K. Chakravartty

Mechanical Metallurgy Division, Bhabha Atomic Research Centre, Mumbai-400-085
*Email: rnsingh@barc.gov.in Tel. +91-22-25593817 FAX: +91-22-25505151

ABSTRACT

Tubes made of Zr-2.5Nb alloy serve as pressure boundary for hot coolant in pressurized heavy water reactors (PHWR). During service the pressure tube material is exposed to an environment comprising of hot coolant, stress, temperature and irradiation resulting in in-service degradation mechanisms like aqueous corrosion, hydride embrittlement and irradiation damage. The fracture toughness parameters are used for safety assessment and residual life estimation of pressure tubes. However, the fracture toughness parameters are reported to be influenced to a varying degree by hydrogen content, temperature and microstructural condition. Though the chemical composition of the Zr-2.5Nb alloy is nearly identical the metallurgical condition of the Zr-2.5Nb tubes varies in different countries and hence in service performance is also reported to vary. The objective of this study was to study the influence of hydrogen content on fracture toughness of heat treated Zr-2.5Nb alloy. The starting material was autoclaved Zr-2.5Nb pressure tube material. Curved compact toughness specimens of width 17 mm were machined from tube pieces gaseously charged with 20, 40, 80 and 100 wppm of hydrogen. These samples were sealed in quartz under 75 torr of He and quenched 843, 873 and 903 °C after soaking for 30 min. Fracture toughness tests were carried out as per ASTM standard E1820-06. At 25 °C autoclaved material showed marginal increase in fracture toughness with increase in hydrogen content. The samples treated at 873 °C showed highest toughness value. The alloy treated at 903 °C was observed to be less susceptible to hydride embrittlement.

INTRODUCTION

Zirconium alloys are extensively used in nuclear thermal power reactors as in-core components like pressure tubes, calandria tubes, fuel cladding tubes, garter springs, channel boxes, instrument guide tubes and for other similar components by virtue of their low neutron absorption cross section, good corrosion resistance, good elevated temperature mechanical properties and adequate irradiation resistance [Glasstone and Sesonske (1998), Cheadle et. al (1982) and Dietz (1994)]. Zr-2.5%Nb alloy in cold worked and stress relieved condition is used as pressure tubes (PT) in Indian Pressurized Heavy Water Reactors (IPHWR) [Lemaignan, and Motta (1994), Fleck et. al (1984) and Singh et. al (2009)]. The PTs are fabricated by hot extrusion process followed by two stage pilgering with an intermediate annealing step, cold working and stress relieving [Singh et. al (2009)]. The microstructure and texture developed during fabrication of PT not only control mechanical properties (such as strength and fracture toughness) but also influence its susceptibility to hydride embrittlement and irradiation induced dimensional changes. Recent work [Coleman (2007) and Griffiths (2002)] has shown that heat-treated Zr-2.5Nb alloy is more resistant to flaw and in-reactor dimensional changes.

In this study fracture toughness parameters such as J_Q, $J_{0.15}$, J_{Max}, $J_{1.5}$, dJ/da, K_Q and CCL were determined as a function of hydrogen content in the range 20 – 100 wppm at ambient temperature. Apart from this, microstructure of the material was varied to obtain various strength levels by helium quenching from three soaking temperatures in the (α+β) phase field viz., 843, 873 and 903 °C. The fracture toughness tests were carried out as per E1820-06 using 17 mm width Curved Compact Tension (CCT). The fracture toughness parameters are used to assess the flaw tolerance capability of the pressure tubes.

EXPERIMENTAL

Material and Specimen

The material used in this study was from double melted, autoclaved, unirradiated Zr-2.5Nb pressure tube of 235 MWe IPHWR. The internal diameter of the tube was 81.5 mm with wall thickness of 3.7 mm. The pressure tube sections of length 100 mm were polished up to 1200 grit emery paper to obtain oxide free surface and subsequently these tube sections were gaseously charged with target hydrogen concentration of 20, 40, 80 and 100 wppm in a modified Sievert's type apparatus [Singh et. al (2003)]. The hydrogen charging was carried out at 363 °C and the charging duration at this temperature was about 1 h for maximum target hydrogen concentration of 100 wppm. The samples charged with lower amount hydrogen were also soaked for one hour at 363 °C so as to subject all the material to the same thermal cycle. Subsequently all the samples were homogenized for 24 h at 400°C to obtain uniform distribution of hydrides. Curved Compact Toughness (CCT) specimens of width 17 mm were machined by EDM wire cutting from these spools. The crack plane was along axial-radial plane to facilitate crack propagation along axial direction of the tube as described elsewhere [Singh et. al (2006)]. The hydrogen charged samples were sealed in quartz capsules under the helium pressure of 75 torr. The sealed samples were helium quenched (cooling in water without breaking the capsule) from three soaking temperature after soaking for 30 minutes. The three soaking temperatures were 843, 873 and 903°C. The duplicate tensile tests were carried out for as received (CWSR) and samples helium quenched from the 843, 873 and 903°C to find out the flow stress which is an input for fracture analysis.

Fracture toughness testing

The CCT samples were fatigue pre-cracked to obtain sharp crack using sinusoidal cyclic loading at a frequency of 10 Hz. The maximum stress intensity factor, K_I, for fatigue pre-cracking, calculated using *equation 1*, was reduced in four steps from the starting value of 15 MPa√m to the final value of 10 MPa√m with the ratio of minimum to maximum load being maintained around 0.1. Fracture toughness tests were carried out as per ASTM E1820-06 method [ASTM E-1820-06]. The crack length was determined using direct current potential drop (DCPD) technique [Singh et. al (2006), Davies and Sterns (1986) and Huang (1993)]. Due to curvature of the CCT specimens tapered pins were used to obtain uniform crack front across the thickness of the specimen.

$$K_I = \frac{P_Q}{BW^{1/2}} f(a/W) \tag{1}$$

where

P_Q = applied load (N),
B = specimen thickness (m),
W = specimen width (m),
a = crack length (m) measured from the load line of the CCT specimens

and

$$f\left(\frac{a}{W}\right) = \frac{\left[2+\frac{a}{W}\right]\left[0.886+4.64\frac{a}{W}-13.32\left(\frac{a}{W}\right)^2+14.72\left(\frac{a}{W}\right)^3-5.6\left(\frac{a}{W}\right)^4\right]}{\left(1-\frac{a}{W}\right)^{3/2}} \tag{2}$$

The value of after fatigue pre-cracking was about 0.5. An Instron make screw driven UTM was used to pull the fatigue pre-cracked specimen in tension to facilitate mode I crack propagation on the axial-radial plane along axial direction of the tube. The specimens were pulled at 0.5 mm/min. The crack

growth was monitored using direct current potential drop technique [Singh et. al (2006), Davies and Sterns (1986) and Huang (1993)].]. A constant DC current of 6 Amperes was used for all specimens. The DCPD output was measured during entire test duration using 0.2 mm diameter platinum wires spot-welded to the crack opening within 1 mm of the each side of the notch. The DCPD and thermocouple outputs were continuously recorded on a 12-channel video graphic recorder. Both fatigue crack length and the final crack length subsequent to fracture toughness testing were calculated from the nine equi-spaced readings along the crack front as per ASTM E1820-06 standard [ASTM E-1820-06]. The crack length was linearly interpolated based on initial and final crack lengths measured optically.

Computations

In this investigation the elastic and plastic component of J are calculated separately. The elastic component was computed from the load and using elastic constant of the material while the plastic component of J was calculated by normalizing the plastic area under the load (P) vs. load line displacement (LLD) (corrected for crack growth as given in ASTM-1820) curve. The procedure for computing J is given below [ASTM E-1820-06]:

$$J_{(i)} = J_{e(i)} + J_{pl(i)} \tag{3}$$

where, J_e = Elastic part of J-integral corresponding to i^{th} data point on load- displacement curve,
J_{pl}= Plastic part of J-integral corresponding to i^{th} data point on load-displacement curve. The J_e is calculated as:

$$J_{e(i)} = \frac{K_{(i)}^2 (1-\nu^2)}{E} \tag{4}$$

where, $K_{(i)}$ = the value of K computed as equation (1) corresponding to i^{th} data point on load-displacement curve, ν = the poison's ratio = 0.436-4.8*10^{-4}(T-300) [Puls (1990)], E = the elastic constant = 95900-57.4(T-273) MPa [15] and J_{pl} is calculated as:

$$J_{pl(i)} = \left[J_{pl(i-1)} + \frac{\eta_{(i-1)}}{b_{(i-1)}} \frac{(A_{pl(i)} - A_{pl(i-1)})}{B} \right] \left[1 - \gamma_{(i-1)} \frac{(a_{(i)} - a_{(i-1)})}{b_{(i-1)}} \right] \tag{5}$$

where

$$\eta_{(i-1)} = 2.0 + \frac{0.522 b_{(i-1)}}{W} \tag{6}$$

$$\gamma_{(i-1)} = 1.0 + \frac{0.76 b_{(i-1)}}{W} \tag{7}$$

b = the remaining unbroken ligament

In equation (5) the quantity $A_{pl(i)}$-$A_{pl(i-1)}$ is the increment of plastic area under the force vs. corrected plastic load line displacement record between lines of constant displacement at points i-1 and i.

$$A_{pl(i)} - A_{pl(i-1)} = \frac{(P_{(i-1)} + P_{(i)})(\delta_{(i)} - \delta_{(i-1)})}{2} \tag{8}$$

The various fracture toughness parameters were determined from the J-R curve generated for as-received as well as HeQ samples containing 20, 40, 80 and 100 wppm of hydrogen. For recording hydride morphology, the specimens were sectioned along radial-circumferential and radial-axial plane of the pressure tube. Standard metallographic technique was followed to reveal the hydride microstructure, its morphology and distribution. For optical microscopy the specimens were etched in a solution of HF: HNO3:H2O::2:9:9 for 15 seconds.

RESULTS AND DISCUSSION

Microstructure

As Received (CWSR)

The current fabrication route of CWSR Zr-2.5 wt. % Nb pressure tubes produces a two phase microstructure of strongly textured and elongated (in axial direction) α-grains surrounded by very thin nearly continuous β-phase network along the grain-boundaries [Srivastava (1995)]. The α-grains, possess HCP structure, with basal poles predominantly aligned in the circumferential (transverse) or radial direction of the tubes. Crystallographically permitted orientation of the hydride platelets in Zr-2.5Nb pressure tube alloy [Northwood and Kosasih (1983)].

The microstructural features of hydrides on RC plane of the Zr-2.5Nb pressure tube material, charged with target hydrogen (a) 20 (21), (b) 40 (53), (c) 80 (86) and (d) 100 (143) wt. ppm of hydrogen, are shown in Figure 1. The figures shown in bracket are estimated hydrogen content of the samples using IGF technique. This figure shows that for CSWR material in the as-hydrided condition, the traces of the hydride platelets (dark lines) are oriented along the circumferential direction only. These hydrides are called circumferential hydrides**.**

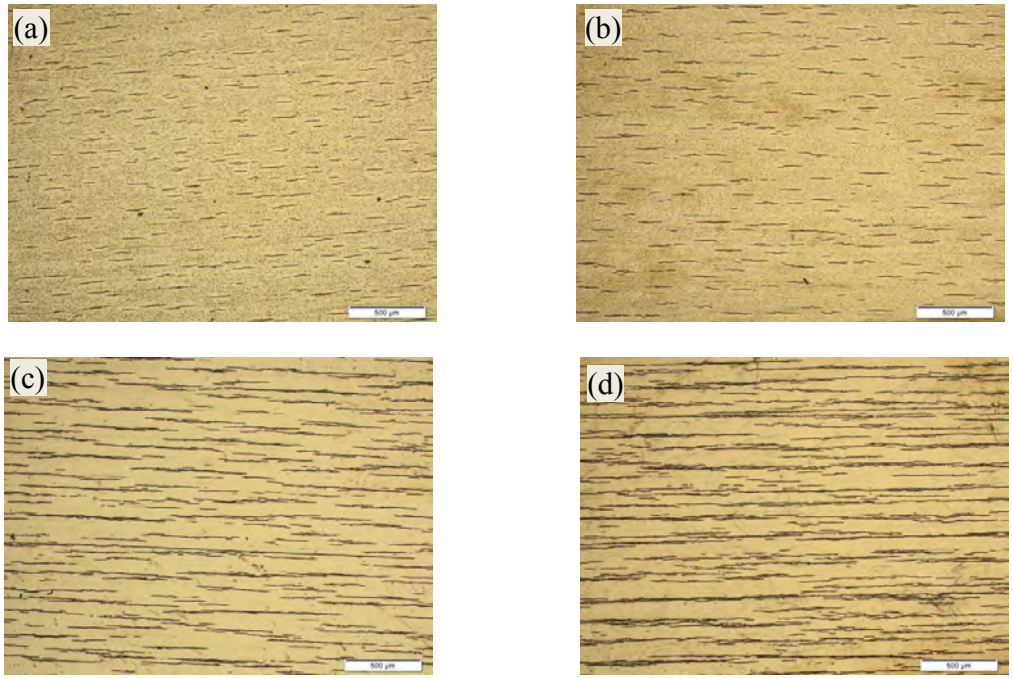

Figure 1. Optical micrographs showing hydrides (dark lines) on RC plane of the Zr-2.5Nb pressure tube material, charged with (a) 20, (b) 40, (c) 80 and (d) 100 wt. ppm of hydrogen.

Helium Quenched

Figure 2 shows microstructure of Zr-2.5Nb alloy helium quenched from (a) 843°C/30 min, (b) 873°C/30 min and (c) 903°C/30 min. In case of helium quenched samples area fraction of α phase decreases with increase in temperature. This is due to fact that as temperature increases volume fraction of α phase decreases and β phases increases. The grain size of α phase decreases with increase in soaking temperature. The grain size of β phase was observed to increase with increase in temperature due to grain-coarsening facilitated by enhanced diffusivity at higher temperature. During cooling the β phase existing at soaking temperature transforms to widmanstatten structure which is not readily resolved under optical microscope.

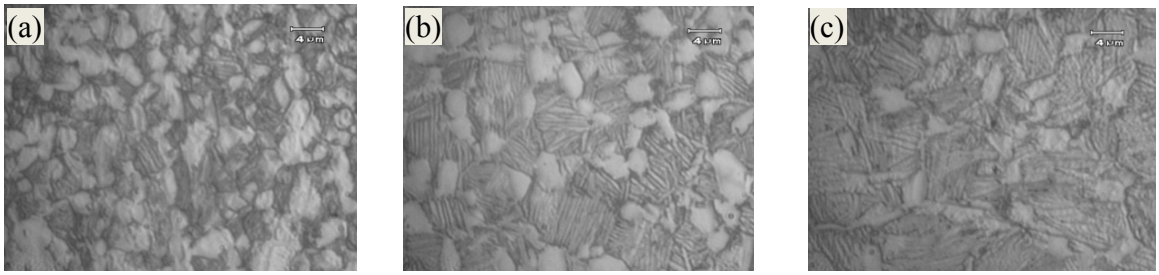

Figure 2. Microstructure of Zr-2.5Nb alloy helium quenched from (a) 843°C/30 min, (b) 873°C/30 min and (c) 903°C/30 min. With increase in soaking temperature fraction and size of β phase increases while α grain size is unaffected by soakting temperature.

Tensile Properties

The tensile data as required input to fracture analysis is given in Table 1. The yield strength (YS), ultimate tensile strength (UTS) and flow stress (FS) of as-received material are greater than that of heat-treated materials and decreases with increase in soaking temperature. The uniform plastic strain (e_{up}) and total plastic strain of (e_{tp}) as-received materials is less that of heat-treated materials. In case of heat-treated materials, the values of e_{up} increases slightly with increase in soaking where as e_{ut} decreases with increase in soaking temperature.

Table 1: Tensile properties of as received and Helium Quenched (HeQ) samples

S. No.	Treatment	YS (MPa)	UTS (MPa)	FS (MPa)	e_{up} (%)	e_{tp} (%)
1	As Received	558	811	685	6.4	16.1
2	843 ^{o}C/30 min./HeQ	534	671	603	7.8	21.9
3	873 ^{o}C/30 min./HeQ	502	626	564	8.2	22.2
4	903 ^{o}C/30 min./HeQ	508	606	557	9.1	19.7

Fracture toughness tests

Initially 32 samples were tested in this work, with duplicate samples for each condition. For certain conditions crack growth in bursts were observed. A typical fractograph showing different regions of crack growth in burst is depicted in Figure 3. Because of brittle and sudden failure in elastic region, J parameters could not be calculated for 12 samples. 12 more tests were carried out for the condition in which the samples failed in brittle manner. During the repeat tests also the samples which failed in brittle manner showed identical behavior. All samples with 20 ppm hydrogen content could be tested

successfully. Also all as received samples could be tested successfully irrespective of hydrogen content. Out of 8 samples of 40 ppm hydrogen content, 5 samples did not meet the J test criteria. The 40 ppm hydrogen containing sample which did not meet the J-test criteria were as follows: two samples each of He quenched from 843 °C and 873 °C and one sample He quenched from 903 °C after a soaking of 30 min. Also both the 80 ppm hydrogen containing samples that were He quenched from 843 °C after 30 min. soaking did not meet the test criteria. Out of 8 samples of 100 ppm hydrogen content, 5 samples did not meet the test criteria. The samples that showed brittle behavior were those HeQ from 843 °C and 873 °C. Though, one of the samples HeQ from 903 °C also exhibited brittle behavior.

The test matrix mentioning valid or invalid tests is given in Table 2

Table 2. Test Matrix

		Hydrogen Content			
Treatment	Sample No.	20	40	80	100
AR	1st	Valid	Valid	Valid	Valid
	2nd	Valid	Valid	Valid	Valid
He/843 °C	1st	Valid	Invalid	Invalid	Invalid
	2nd	Valid	Invalid	Invalid	Invalid
He/873 °C	1st	Valid	Invalid	Valid	Invalid
	2nd	Valid	invalid	Valid	Invalid
He/903 °C	1st	Valid	Valid	Valid	Invalid
	2nd	Valid	Invalid	Valid	Valid

It may concluded from the test matrix that for the HeQ samples, as the hydrogen content increases and soaking temperature decreases, probability for sample to fail in brittle manner increases. So it can be said that micro-structural parameters also play important role in brittle behavior of the Zr-2.5Nb alloy. As the soaking temperature increases, fraction of β-phase increases. During quenching, the β phase transforms to widmanstatten α or martensite phase depending upon the rate of cooling. For the helium quenching from the soaking temperatures 843-903 °C it is reported that widmanstatten α forms in this alloy. For faster cooling rates, which is possible for samples quenched from higher soaking temperatures, the sub-structure of widmanstatten structure will be finer.

Thus it may be concluded that samples having more fraction of β phase at the soaking temperature, i.e., those quenched from higher soaking temperature are less susceptible to hydrogen embrittlement. This is expected due to finer widmanstatten structure forming in samples quenched from higher soaking temperature. So as soaking temperature increases, sample is less susceptible to hydrogen embrittlement.

Variation of K_Q

For different heat treatment conditions, variation of K_Q with hydrogen content is shown in Figure 4a. For as received samples, value of K_Q increased marginally with increase in hydrogen content. For heat-treated samples K_Q decreased with increase in hydrogen content. The rate of decrease of K_Q with hydrogen content decreased with increase in soaking temperature (Figure 4a). For different hydrogen content, variation of K_Q with heat treatment conditions is shown in Figure 4b. Except for 20 ppm samples, as received samples have higher K_Q value than heat-treated samples (Figure 4b). For 20 ppm samples, value of K_Q was constant between soaking temperature of 843 to 873 °C and then dropped from 873 °C to 903 °C. For 40 ppm samples, K_Q was constant with soaking temperature. For 80 ppm samples, K_Q first

increased as the soaking temperature was increased from 843 to 873 °C and then decreased with further increase in soaking temperature. For the samples containing 100 ppm increase in K_Q with soaking temperature was observed. The very interesting fact about these graphs is that as hydrogen content is increasing the maximum K_Q is shifting toward higher soaking temperature. It means that hydrogen is also affecting the toughness of heat-treated samples. Samples having highest toughness for a given heat-treatment condition show more number of axial splits on their respective fractographs. So it may be concluded that these dark lines are responsible for higher toughness values. The slope obtained by linear regression analysis of the K_Q vs. C_H plots suggested that as the soaking temperature increased, the magnitude of slope of the curve decreased linearly (Figure 4a). It signifies that as soaking temperature increases, susceptible to hydrogen embrittlement decreases.

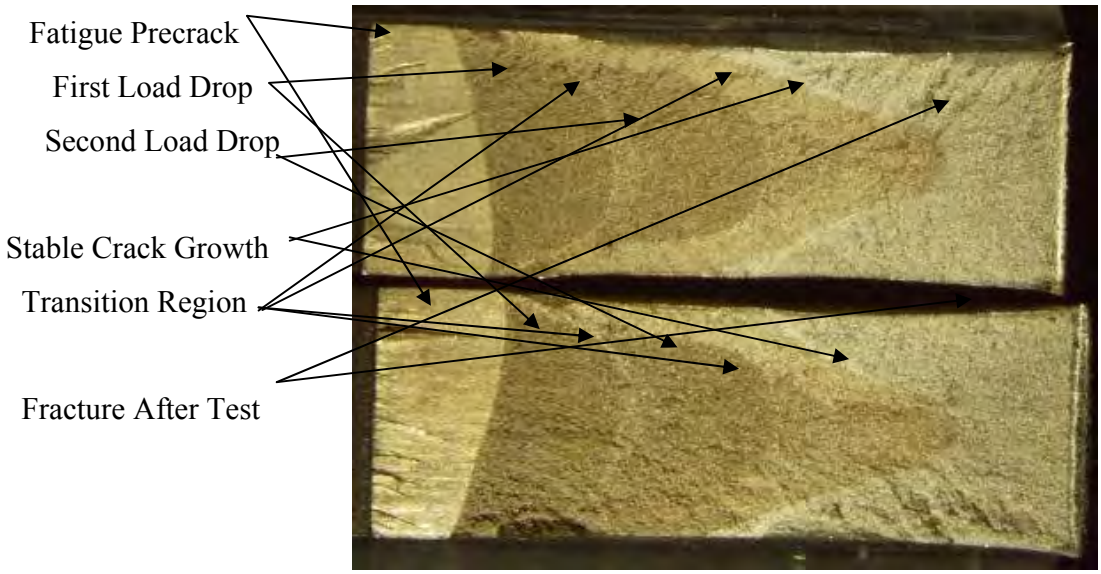

Figure 3. Typical fractographs as observed under Stereo Microscope showing Different Regions of unstable crack growth

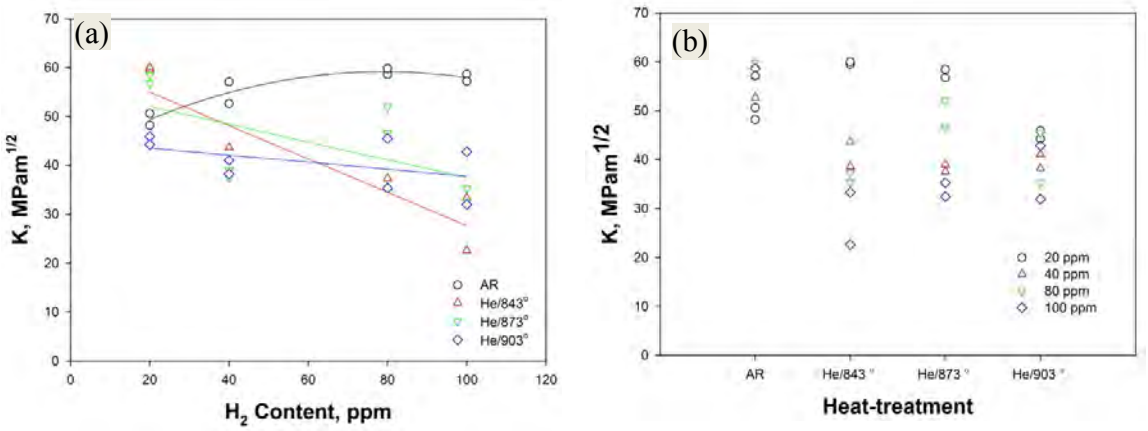

Figure 4. Variation of K_Q with (a) hydrogen content and (b) heat-treatment condition

Variation of J Parameters

The fracture toughness parameters such as J_Q, $J_{0.15}$ and J_{Max} , $J_{1.5}$ and *dJ/da* were determined for each conditions of testing. For the sake of clarity, of the various fracture parameters we report only the variations of J_{Max} and *dJ/da* with hydrogen content and heat-treatment condition. For different heat treatment conditions, variation of J_{Max} and dJ/da with hydrogen content is shown in Figure 5. For all hydrogen content, the values of J_{Max} and dJ/da of heat-treated samples are greater than that of as-received samples (Figure 5a and 5b). For as received samples, value of J_{Max} increased marginally with increase in hydrogen content (Figure 5a), while dJ/da decreased marginally with increase in hydrogen content (Figure 5b). For all heat-treated samples, value of J_{Max} and dJ/da decreased with increase in hydrogen content (Figure 5a and 5b).

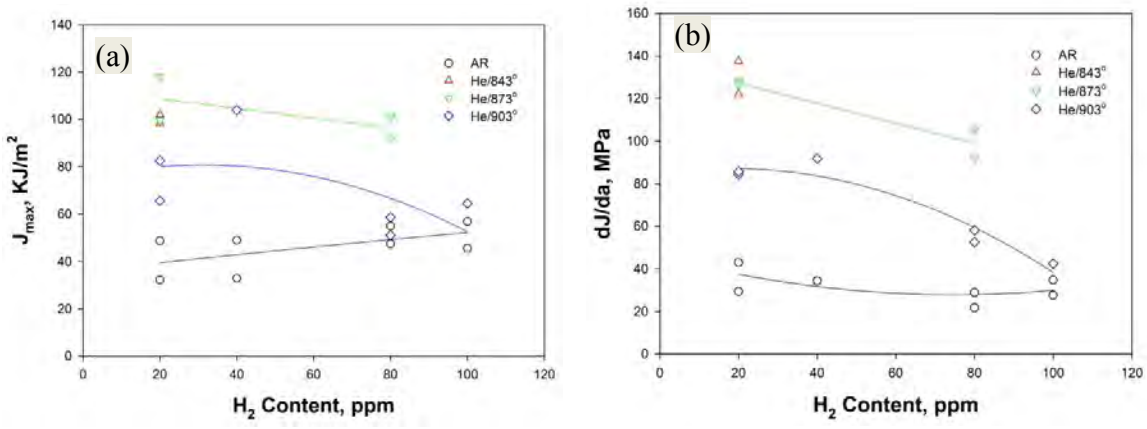

Figure 5. Variation of (a) J_{Max} and (b) dJ/da with hydrogen content for as-received and helium quenched samples

For different hydrogen content, variation of J_{Max} and dJ/da with heat treatment conditions is shown in Figure 6. For all hydrogen content, the values of J_{Max} and dJ/da of all heat-treated samples are greater than that of as-received samples (Figure 6a and 6b). The samples containing 20 ppm hydrogen showed the maximum J_{Max} corresponding to soaking temperature of 873^o afterwards the value of J_{Max} decreased with increase in soaking temperature (fig 6a). The samples helium quenched from 843 and 873^o have nearly same J_{Max} values (fig 6a). The J_{Max} values of samples helium quenched from 873^{o}C is nearly double as compared to as-received samples. The dJ/da showed similar behavior for samples containing 20 ppm hydrogen (fig 6b). The samples containing 40 ppm hydrogen and helium quenched from 843 °C and 873 °C failed to meet valid J test. As compared to as-received samples, sample helium quenched from 903 °C has higher value of J_{Max} and dJ/da. The crack propagation parameters increased two fold after heat-treatment. The samples containing 80 ppm hydrogen and helium quenched from 843 °C failed to meet valid J test criteria. Value of crack propagation parameters i.e. J_{Max}, and dJ/da of heat-treated samples are higher than as-received samples (figs.6a and 6b). All the fracture parameters decreased drastically with increase in soaking temperature from 873 °C to 903 °C. The dJ/da shows maximum sensitivity to treatment. The samples containing 100 ppm and helium quenched from 843 °C and 873 °C failed to meet valid J test criteria. As compared to as-received samples, sample helium quenched from 903 °C has higher value of crack propagation parameters i.e. J_{Max}, and dJ/da (figs 6a and 6b).

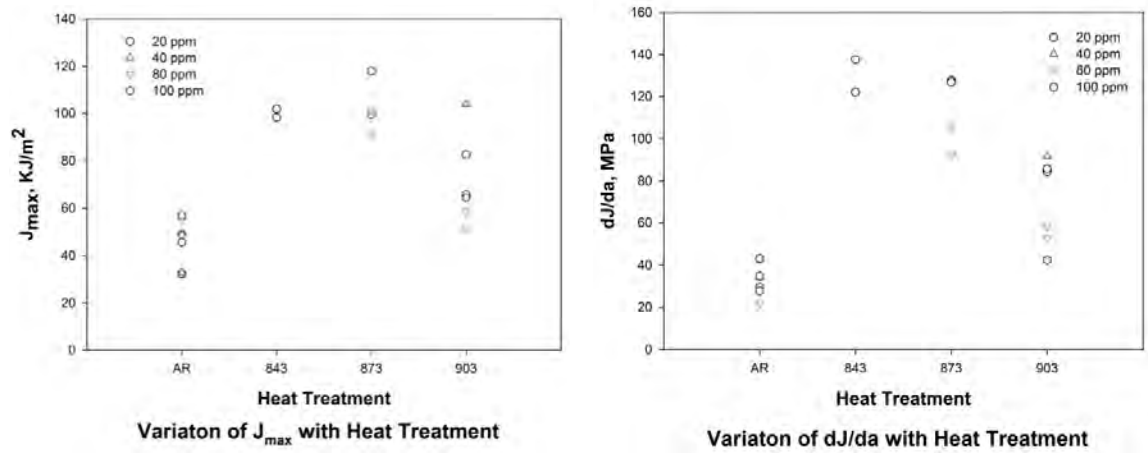

Figure 6 Variation of (a) J_{Max} and (b) dJ/da with heat-treatment condition for different hydrogen content samples

CONCLUSIONS

Fracture toughness parameters of double melted cold worked and stress relieved Zr-2.5Nb pressure tube material and helium quenched from 843, 873 and 903 ^{o}C were evaluated as a function of hydrogen content (20-100 wppm). On the basis of the results obtained following conclusion can be drawn**:**

1. Samples helium quenched from lower soaking temperature and having higher hydrogen content may fail in brittle manner.

2. For as received sample, K_Q increases with increase in hydrogen content and it value saturates at 100 ppm. For other samples K_Q was observed to decrease with increase in hydrogen content. The magnitude of slope of the K_Q vs. C_H plot decreases with increase in soaking temperature suggesting decrease in susceptibility of this alloy to hydrogen embrittlement with increase in soaking temperature.

3. The fracture toughness parameters J_{Max} and dJ/da of all heat-treated samples were greater than that of as received samples and is maximum for samples helium quenched from 873 ^{o}C and decreased drastically after that.

REFERENCES

ASTM Standard, E-1820-06.

Cheadle, B. A., Coleman, C. E. and Litcht, H. (1982). "CANDU-PHW Pressure Tubes : Their manufacture, inspection and properties," *Nucl. Tech.* 57, 413-425.

Coleman, C., Griffiths, M., Grigoriev V., Vladimir K., Rodchenkov B., and Markelov V. (2007) "Mechanical Properties of Zr-2.5Nb Pressure Tubes Made from Electrolytic Powder" *Journal of ASTM International*, 4(10)1-23.

Davies, P. H. and Sterns, C. P. (1986). "Fracture toughness testing of zircaloy -2 pressure tube material with radial hydrides using direct-current potential drop", in: J.H. Underwood, R. Chait, C.W. Smith, D.P. Wilhem, W.A. Andrews and J.C. Newman (Eds.) *ASTM STP* 905, 379.

Dietz, W. (1994). *Structural Materials, Materials Science & Techno. A Comprehensive Treatment*, eds. R. W. Cahn, P. Haasen & E. J. Kramer, 10B, Nuclear Materials, Chapter 8, 53.

Fleck, R. G., Price, E. G., and Cheadle, B. A. (1984). "Pressure Tube Development for CANDU Reactors" *Zirconium in Nuclear Indusatry. ASTM STP* 824, 88-105.

Glasstone, S. and Sesonske, A. (1988). *Nuclear Reactor Engineering*, 3rd edition, CBS publishers and Distributors, Delhi (India).

Griffiths, M., Davies, W. G., Causey, A. R, Moan, G. D., Holt, R. A., and Aldridge, S. A. (2002). "Variability of In-Reactor Diametral Deformation for Zr-2,SNb Pressure Tubing," *Zirconium in the Nuclear Industry: Thirteenth International Symposium, ASTM STP 1423,* G. D. Moan and P. Rudling, Eds., ASTM International, West Conshohocken, PA,796-810.

. Huang, F. H. (1993). "Fracture toughness evaluation for zircaloy-2 pressure tubes with the electric-potential method", *ASTM Intl. Symp. On Small specimen test techniques applied to nuclear reactor vessel thermal annealing and plant life extension*, New Orlearns, LA, USA.

Lemaignan, C. and Motta, A. T. (1994). "Zirconium alloys in nuclear applications", *ibid* 10B Chapter 7, 1.

Northwood, D. O., and Kosasih, U. (1983). "Hydrides and delayed hydrogen cracking in zirconium and its alloys," *Intl. Metals Rev.*, 28(2) 92-121.

Puls, M. P. (1990). "Effects of Crack Tip Stress States and Hydride-Matrix Interaction Stresses on Delayed Hydride Cracking" *Metall. Trans. A* 21A 2905-2917.

Singh, R.N., Ståhle, P., Chakravartty, J.K., Shmakov, A.A. (2009) "Threshold stress intensity factor for Delayed hydride cracking in Zr-2.5%Nb pressure tube alloy" *Mater. Sc. and Engg. A*, 523, 112-117.

Singh, R. N., Kishore, R., Mukherjee, S., Roychowdhury, S., Srivastava, D., Gopalan, B., Kameswaran, R., Sheelvantra, S.S., Sinha, T. K., De, P. K. and Banerjee, S. (2003). "Hydrogen charging, hydrogen contentanalysis and metallographic examination of hydride in Zirconium alloys", *BARC report No. BARC/2003/E/034*, 1-45.

Singh, R. N., Ståhle, P. and Srinivasan, N. S., (2006) "Influence of Hydrogen Content on Axial Fracture Toughness Parameters of Zr-2.5Nb Pressure Tube Alloy in the Temperature Range of 306-573 K" *Proc. of ICAPP '06* Reno, NV USA, June 4-8, 2006, Paper 6138.

Srivastava, D., Dey G.K. and Banerjee, S. (1995). "Evolution of microstructure during fabrication of Zr-2.5 Wt pct Nb alloy pressure tubes, *Metall. Trans. A,* 26A, 2707-2718.